Size effects and dielectric behaviour in ferroelectric heterostructures

2006 J. Phys.: Condens. Matter 18 5725

(http://iopscience.iop.org/0953-8984/18/24/013)

INSTITUTE OF PHYSICS PUBLISHING JOURNAL OF PHYSICS: CONDENSED MATTER

J. Phys.: Condens. Matter **18** (2006) 5725–5738 doi:10.1088/0953-8984/18/24/013

Size effects and dielectric behaviour in ferroelectric heterostructures

M Tyunina

Microelectronics and Materials Physics Laboratories, University of Oulu, PL 4500, FI-90014 Oulun Yliopisto, Finland

E-mail: marinat@ee.oulu.fi

Received 3 February 2006
Published 2 June 2006
Online at stacks.iop.org/JPhysCM/18/5725

Abstract

The low-frequency dielectric response of thin-film and bulk ferroelectric or relaxor heterostructures was analysed. For epitaxial crystallographic strain-free thin films of ferroelectric (Ba, Sr)TiO_3 and relaxor $PbMg_{1/3}Nb_{2/3}O_3$, more experimental data supporting the interface layer model were obtained. The combined effects of properties and thicknesses of both the films and electrode layers on the dielectric response were demonstrated using the comparison of the experimental results with the results of estimations. In thin-film heterostructures, the anomalous frequency dispersion of the dielectric permittivity and losses was explained as originating from the joint film–electrode scaling. The study of the interface parameters using the thickness dependence of the permittivity was shown to be incorrect. In bulk relaxors, the relaxor–electrode pair was found to give apparent additional relaxation laws not related to the true dielectric relaxation. Both in thin-film and bulk heterostructures, a lower-resistivity layer was suggested to exist at the surface of perovskite ferroelectrics and relaxors.

1. Introduction

In the last decade, the size effects in perovskite ferroelectrics (FEs) and relaxors (RFEs) have become a subject of intense research, both theoretical and experimental. In particular, much attention has been paid to thin-film FEs due to their potential for modern device applications [1]. Despite a considerable progress in the field, the results of experimental studies remain scattered and often controversial to the model predictions. In thin-film FE heterostructures, in part this can be related to neglecting a possible influence of the accompanying size effects in electrode layers and combination of the size effects.

One of the most generally observed peculiarities of thin-film FE is the small real part of the dielectric permittivity. It can be smaller than that of the corresponding bulk FEs by an order of magnitude, it decreases with decreasing thickness of FEs, and exhibits a broad

peak in the temperature dependence. Usually an interface layer model [2, 3] satisfactorily describes this behaviour. Also both clamping and strain in thin-film FEs can result in a reduced permittivity [4]. For a correct analysis of the reduced permittivity, one needs to distinguish and separate the contributions. On the other side, the loss factor of thin-film FEs is relatively large. At all temperatures, the permittivity and loss factor strongly vary with frequency even in the low-frequency range [5, 6]. Neither the interface model, nor any other model, can explain this.

The purpose of the present work was to demonstrate the combined effects of properties and thicknesses of both FE and electrode layers on the dielectric response measured in the vertical thin-film FE heterostructure. The dielectric behaviour of thin-film FE and RFE heterostructures was experimentally studied and analysed, providing more data in support of the interface model. Considering this, the low-frequency dielectric properties of thin-film FEs with thin-film electrodes were estimated, that made it possible to explain the observed large losses and dielectric dispersion. The low-frequency dielectric response of the heterostructure of bulk RFEs was estimated, too. A possible appearance of additional relaxation laws, which are not related to the true dielectric relaxation in RFEs, was shown. Based on the comparison of the experimental results with the results of estimations in thin-film FEs and bulk RFEs, the presence of a lower-resistivity layer at the surface of perovskite FE/RFEs was suggested.

2. Thin-film ferroelectrics and relaxors

Heterostructures of either ferroelectric (FE) or relaxor ferroelectric (RFE) thin films were grown by *in situ* pulsed laser deposition on (100) MgO crystal substrates using an oxide $La_{0.5}Sr_{0.5}CoO_3$ (LSCO) bottom electrode [6, 7]. For the present study, thin films of the best studied 'typical' FE $Ba_{0.4}Sr_{0.6}TiO_3$ (BST) and RFE $PbMg_{1/3}Nb_{2/3}O_3$ (PMN) were prepared. The epitaxial quality of the heterostructures and the presence of pure perovskite phase with [100] crystal orientation in RFE/FE films were evidenced by the room-temperature x-ray diffraction [6, 7]. To estimate the possible interface contribution, only the films with the lattice parameters similar to those of the bulk prototypes, or crystallographic strain-free films, were selected. For the dielectric characterization of the films, vertical capacitor heterostructures with Pt top electrode pads were formed by pulsed laser deposition of Pt through a mask. In such heterostructures, the capacitance C and loss factor $\tan\delta$ were measured at a small amplitude of ac electric field as a function of frequency $f = 10^2$–10^6 Hz and temperature $T = 90$–650 K using an HP 4284A LCR meter. The real part of the dielectric permittivity ε' was estimated from the parallel plate capacitor model: $C = \varepsilon_0\varepsilon' S/d_F$, where S is the area of the top electrode and d_F is the thickness of the PMN or BST film.

In a BST thin-film capacitor with $d_F = 250$ nm, the temperature dependence of the permittivity ε' (figure 1(a)) was similar to that typically observed in thin-film FEs. Namely, compared to ceramic BST, the dielectric peak was broader and the maximum permittivity was considerably smaller. An important feature was the frequency dispersion of the permittivity seen in the whole temperature range. In FE thin films, such a low frequency dielectric dispersion has not often been studied and reported.

The temperature dependence of the inverse permittivity $1/\varepsilon'$ (figure 1(b)) exhibited a linear behaviour at temperatures above 250 K, in agreement with the Curie–Weiss law: $\varepsilon' = c/(T - \Theta)$, where c is the Curie constant and Θ is the Curie temperature. The Curie constant determined from the best linear fits appeared to be frequency independent and equal to $c \sim 10^5$ K, close to that in ceramic FEs. However, the Curie temperature, also determined from the linear fits, did depend on frequency and it varied in the range from $\Theta = 140$ K at 0.5 kHz to $\Theta = 125$ K at 50 kHz. Moreover, the temperature Θ was lower than that of the dielectric maximum: $T_m = 178$ K.

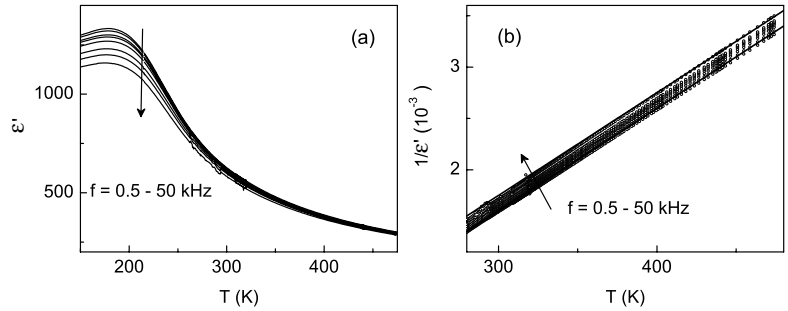

Figure 1. The real part of the dielectric permittivity ε' (a) and the corresponding inverse permittivity $1/\varepsilon'$ (b) as a function of temperature T determined in $Ba_{0.4}Sr_{0.6}TiO_3$ thin film heterostructure at frequencies $f = 0.5$–50 kHz. The direction of increase of f is shown by arrows. The straight lines in (b) are fits to the Curie–Weiss law.

Both such an unphysical temperature $\Theta < T_m$ and small permittivity can be explained in terms of the often applied interface layer model [2, 3]. According to the model, a thin low permittivity dielectric layer at the film–electrode interface is connected in series to the film. For the interface layer with small thickness $d_i \ll d_F$ and low permittivity $\varepsilon'_i \ll \varepsilon'_F$, the permittivity ε' of the thin-film heterostructure can be described by

$$\frac{1}{\varepsilon'} \cong \frac{1}{\varepsilon'_F} + \frac{1}{\varepsilon'_{int}}, \tag{1}$$

where ε'_F is the permittivity of the film material, and ε'_{int} is equal to

$$\varepsilon'_{int} = \frac{\varepsilon'_i}{d_i} d_F. \tag{2}$$

For the high-temperature Curie–Weiss behaviour of the film material $\varepsilon'_F = c/(T - \Theta_F)$, where Θ_F is the true Curie temperature of the film, the Curie–Weiss law in the thin-film heterostructure can be presented by $\varepsilon' = c/(T - \Theta)$, where the temperature Θ can be found using expression (1):

$$\Theta = \Theta_F - \frac{c}{\varepsilon'_{int}}. \tag{3}$$

It is possible to show that ε'_{int} does not noticeably vary with temperature [5]. In thin-film heterostructures, the small permittivity ε' and the low Curie temperature Θ can be explained by the interface effect (expressions (1) and (3)).

In the BST thin-film heterostructure (figure 1(b)), the normalized permittivity of the interface layer ε'_i/d_i could be estimated assuming that the Curie temperature of the film Θ_F was close to the temperature T_m of the dielectric maximum: $\Theta_F \cong T_m$, and, respectively, ε'_{int} was approximately equal to $\varepsilon'_{int} \cong c/(T_m - \Theta)$. Such an estimation gave $\varepsilon'_i/d_i = 8.3$–7.5 nm^{-1} in the frequency range $f = 0.5$–50 kHz. The obtained magnitude of $\varepsilon'_i/d_i \sim 10$ nm^{-1} was consistent with the previous experiments and modelling [8, 3]. Applying expression (1) with the found ε'_i/d_i resulted in the permittivity of BST film $\varepsilon'_F \approx 4000$ at temperatures around T_m.

In RFEs, the Curie–Weiss behaviour can be observed at very high temperatures exceeding T_m by 150–300 K. In RFE thin-film heterostructures, the Curie–Weiss behaviour has been found [5] to possess similarities with that in BST heterostructures (figure 1(b)). The Curie constant was close to c in the bulk prototype, while the temperature Θ was frequency dependent and relatively low.

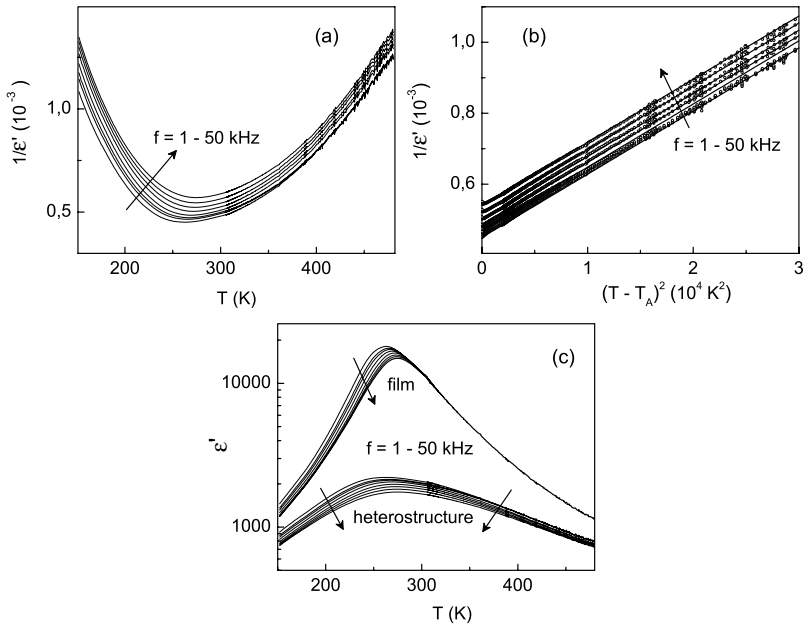

Figure 2. The inverse permittivity $1/\varepsilon'$ (a) as a function of temperature T and (b) as a function of the square of the reduced temperature $(T - T_A)^2$ determined in $PbMg_{1/3}Nb_{2/3}O_3$ thin-film heterostructure at frequencies $f = 1$–50 kHz. The straight lines in (b) are fits to the scaling law. (c) The real part of the dielectric permittivity ε' measured in the heterostructure and reconstructed in the film of $PbMg_{1/3}Nb_{2/3}O_3$. The direction of increase of f is shown by arrows.

For numerous bulk RFEs in the broad range of temperatures $T > T_m$ around T_m, the scaling of the dielectric peak has been empirically derived [9]:

$$\frac{\varepsilon'_A}{\varepsilon'_F} = 1 + \frac{(T - T_A)^2}{2\delta^2}, \tag{4}$$

where ε'_A, T_A, and δ are parameters, and ε'_A has the meaning of the maximum static permittivity. In the thin-film heterostructure of RFE PMN with $d_F = 300$ nm, the inverse permittivity $1/\varepsilon'$ was analysed as either a linear (figure 2(a)) or a square (figure 2(b)) function of temperature.

The Curie–Weiss behaviour was not detected even at temperatures as high as 500–600 K (figure 2(a)). A good linear fit to $1/\varepsilon' \propto (T - T_A)^2$ was found in the temperature range 255–500 K (figure 2(b)). The temperature $T_A = 256$ K was in agreement with that in bulk PMN. The linear fits $1/\varepsilon' \propto (T - T_A)^2$ had similar slopes at different frequencies, but they were moving along $1/\varepsilon'$-axis with increasing frequency (figure 2(b)). Such a peculiar behaviour was consistent with the interface layer model. Using expressions (1) and (4), the scaling law for the permittivity in the heterostructure can be presented in the form

$$\frac{1}{\varepsilon'} = \frac{1}{\varepsilon'_A} + \frac{1}{\varepsilon'_{int}} + \frac{(T - T_A)^2}{2\delta^2\varepsilon'_A} = A + B\,(T - T_A)^2\,, \tag{5}$$

where the fitting coefficient A is determined by the interface

$$A \approx \frac{1}{\varepsilon'_{int}} \tag{6}$$

due to large $\varepsilon'_A \approx 20\,000$ [9]. Also both the frequency dependence of A and frequency independent B can confirm the validity of (6).

In PMN heterostructures, the normalized permittivity of the interface layer ε_i'/d_i was estimated using the best linear fits $1/\varepsilon' \propto (T - T_A)^2$ and expression (6). For the frequencies 1–50 kHz, the obtained ε_i'/d_i was in the range of 11–9.2 nm^{-1}, respectively, close to that in BST heterostructure. The permittivity of PMN film ε_F' was reconstructed using expression (1) with the found ε_i'/d_i (figure 2(c)). The reconstructed $\varepsilon_F'(f, T)$ of thin-film PMN resembled that of bulk PMN [10].

Thus, the dielectric permittivity of FE and RFE thin-film heterostructures could be described in terms of the interface layer model. The normalized permittivity of the interface layer was found to be about 10 nm^{-1}. The reconstructed permittivity of thin films agreed with that of the bulk prototypes.

The main physical reason for the interface layer model is the boundary condition for polarization. At the surface of the film (or at the film–electrode interface) the polarization P differs from that in the volume (or body) of the film. The boundary condition can be formulated as $\frac{dP}{dz}|_{z=\pm\frac{d_F}{2}} = 0$ and $P|_{z=\pm\frac{d_F}{2}} = 0$ (or certain P_0) [3, 11]. The polarization is distributed across the thickness of the film [3, 11]. In the interface model, the resulting distribution of polarization is roughly approximated by a step-like function, including a lower-permittivity part near the surface (interface layer with ε_i') and a larger-permittivity part in the body of the film (film with ε_F'). The minimum thickness d_i of such an interface layer corresponds to the correlation length for polarization [3]. It should be emphasized that the interface layer model does not suggest a real presence of the low-permittivity dielectric, which differs from the body of the FE film either structurally, or compositionally. Also with decreasing thickness of FE, both the maximum polarization in the body of the film and the distribution of polarization can change, resulting in the corresponding change of the interface parameters. These considerations have to be taken into account in any experimental search [8] for the interface layer.

At the interfaces of the real thin-film heterostructures, the peculiarities of microstructure such as dislocations, deviations from stoichiometry, and others, and possible contact barriers can exist. Moreover, the microstructure of the film can be thickness dependent. Also FE films can contain imperfections such as grains, grain boundaries, and point defects, affecting the permittivity. These factors make it even more difficult to use the thickness dependence of permittivity for determining the interface layer parameters. In epitaxial crystallographic strain-free films, the suggested analysis of the high-temperature dielectric behaviour seems to be a satisfactory method of experimental estimation of the interface parameters.

Although numerous experimental results (including those in figures 1 and 2) support the interface layer model, the behaviour of the permittivity ε_i' appeared to be controversial. The permittivity ε_i' has been found to be temperature independent, but to vary with frequency. To understand the origin of the frequency dispersion of ε_i' the model of the thin-film capacitor was considered in more detail.

3. Frequency dependence of the dielectric response of FE thin-film heterostructures

Usually, a parallel plate FE sample is presented as an ideal capacitor which can be described as a series connection of capacitance $C = \varepsilon_0\varepsilon' S/d_F$ and resistance $R = d_F/(S\omega\varepsilon_0\varepsilon'')$, where $\omega = 2\pi f$ and ε'' is the imaginary part of the dielectric permittivity. Respectively, impedance Z^* of such a capacitor is equal to

$$Z^* = Z' - iZ'' = R + \frac{1}{i\omega C}, \tag{7}$$

and the loss factor $\tan\delta$ is determined solely by the dielectric loss:

$$\tan\delta = \frac{Z'}{Z''} = \frac{\varepsilon''}{\varepsilon'}, \tag{8}$$

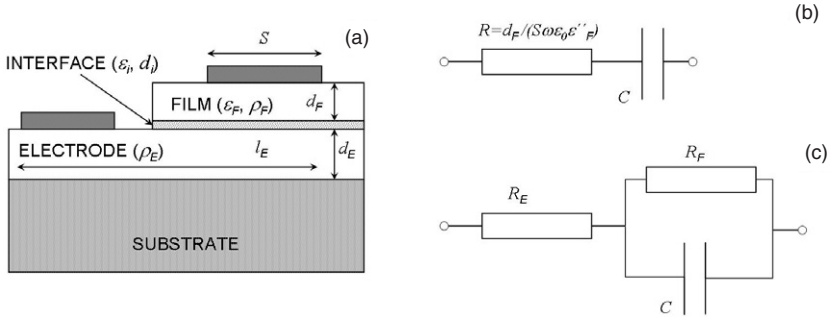

Figure 3. A schematic diagram of the vertical thin-film heterostructure: (a) cross-section, (b) ideal capacitor, and (c) leaky capacitor models. For simplicity, an ideal top electrode and a single interface layer are considered.

$$C = \frac{1}{\omega Z''}. \tag{9}$$

To analyse the dielectric properties of FE, a straightforward analysis of Z^* is performed.

However, the model (7) is valid only for a sufficiently large ohmic resistance of FE and a negligibly small contact resistance. With decreasing thickness d_F of FE, the ohmic resistance decreases. Moreover, FE thin films often possess smaller resistivity ρ_F compared to that of bulk FE. Also in thin-film heterostructures (figure 3(a)), the contact resistance cannot be ignored due to the relatively small thickness d_E of the electrode layers. Thus the real FE thin-film capacitor can be rather described as a parallel connection of capacitance C and a resistance R_F determined by the dielectric loss and conductivity of FE, and a series connection of a resistance R_E determined mainly by the electrode (figure 3(c)).

The impedance Z^* of such a leaky capacitor is

$$Z^* = \left\{ R_E + \frac{R_F}{[1 + (\omega C R_F)^2]} \right\} - i \left\{ \frac{\omega C R_F^2}{[1 + (\omega C R_F)^2]} \right\}, \tag{10}$$

where the resistance R_E can be estimated as

$$R_E = \rho_E \frac{l_E}{(w_E d_E)} \simeq \frac{\rho_E}{d_E} \tag{11}$$

for approximately similar length l_E and width w_E of the electrode. The resistance R_F can be calculated as

$$R_F = \frac{d_F}{S(\omega\varepsilon_0\varepsilon'' + 1/\rho_F)}. \tag{12}$$

The capacitance and the loss factor are related to the impedance in a different manner compared to the expressions (8) and (9):

$$C_m \cong \frac{Z''}{[(Z')^2 + (Z'')^2]}, \tag{13}$$

$$\tan\delta = \frac{R_E + R_F}{\omega C R_F^2} + \omega C R_E. \tag{14}$$

The expression (13) gives the 'measured' capacitance which is directly obtained using an *LCR*-meter. The expression (14) is reduced to (8) and the expression (13) is reduced to (9) for $R_E = 0$ and $1/\rho_F = 0$. In (14) the second term is usually taken into account only at very

high frequencies $f \gg 10^6$ Hz. It is possible to show that in thin-film FEs, this term should be considered even at lower f.

As an example, the impedance, the loss factor, and the 'measured' capacitance C_m of the vertical thin-film heterostructure were estimated using (10)–(14) and assuming the following parameters:

$\varepsilon'_F = 10^2$; 10^3; 10^4; and 10^5 (from FE to RFE);
$\varepsilon''_F/\varepsilon'_F = 10^{-3}$;
$\rho_F = 10^{10}$–10^4 Ω m (from $BaTiO_3$ crystal to semiconductor);
$d_F = 10^{-8}$–10^{-6} m (from 10 nm to 1 μm);
$\rho_E = 10^{-7}$; 2×10^{-6}; and 10^{-4} Ω m (metal, oxide, and polycrystalline oxide film, or 'bad' oxide);
$d_E = 10^{-7}$; 5×10^{-7}; and 10^{-6} m (from 100 nm to 1 μm);
$\varepsilon'_i = 50$;
$\varepsilon''_i = 0$ (ideal dielectric without losses);
$d_i = 5 \times 10^{-9}$ m (5 nm);
$S = 10^{-8}$ m^2 (100 μm × 100 μm);
$f = 1$–10^6 Hz.

To estimate the impedance, the total capacitance C of thin-film FE was calculated as that of the body of the film and interface layer connected in series:

$$C = \varepsilon_0 S \frac{\varepsilon'_F}{[d_F + \varepsilon'_F(\frac{d_i}{\varepsilon'_i})]}. \tag{15}$$

As seen from (15), in thin-film FE with either very large permittivity ε'_F or very small thickness d_F, the capacitance C is limited by the interface capacitance $C_i = \varepsilon_0 S(\varepsilon'_i/d_i)$. Also it can be seen that in thin-film heterostructures the bulk value of permittivity ε'_F can be reached only for a sufficiently large thickness d_F satisfying the condition $d_F \gg \varepsilon'_F(d_i/\varepsilon'_i)$. For example, assuming $\varepsilon'_i/d_i = 10$ nm^{-1}, the permittivity $\varepsilon'_F = 10\,000$ can be obtained for FE thickness in the range of $d_F > 20$ μm, and the maximum permittivity for FE film thickness $d_F = 500$ nm is equal to $\varepsilon'_F = 5000$.

In estimations, all properties of FE film, interface, and electrode layers were taken as frequency independent. The measured permittivity ε' was determined from the 'measured' capacitance C_m as $\varepsilon' = C_m(d_F + d_i)/(\varepsilon_0 S)$. The results of estimations illustrating the influence of different parameters on the measured dielectric response of thin-film FE heterostructures are presented in figures 4–7.

In FE thin-film heterostructures, the loss factor $\tan\delta$ is always larger than the dielectric loss $\varepsilon''_F/\varepsilon'_F$ in FE. With decreasing resistivity ρ_F of the FE film, the factor $\tan\delta$ increases (figure 4(a)) tending to a linear dependence $\log(\tan\delta) \propto -\log(f)$. As follows from (14) for $R_F \gg R_E$, such a low-frequency contribution to the loss is given by $1/(\omega\varepsilon_0\varepsilon'\rho_F)$. The resistivity ρ_F does not affect the 'measured' capacitance C_m (figure 4(b)), but it can result in an artificial increase of ε' (dashed lines in figure 4(b)) if the ideal capacitor (9) is considered. Respectively, applying (8) is not correct.

With either decreasing thickness d_E or increasing resistivity ρ_E of the electrode layer, the measured loss increases (figure 5(a)) tending to a linear dependence $\log(\tan\delta) \propto \log(f)$. Such a frequency dependence of $\tan\delta$ is detectable at frequencies as low as 100 Hz, in contrast to the gigahertz range typical for bulk samples. Due to the effect of electrodes, the measured ε' can drop (figure 5(b)) at higher frequencies.

With increasing permittivity ε'_F of the FE film, the magnitude of increase in losses, which is determined by the electrode, becomes larger. Also the lowest frequency at which this increase

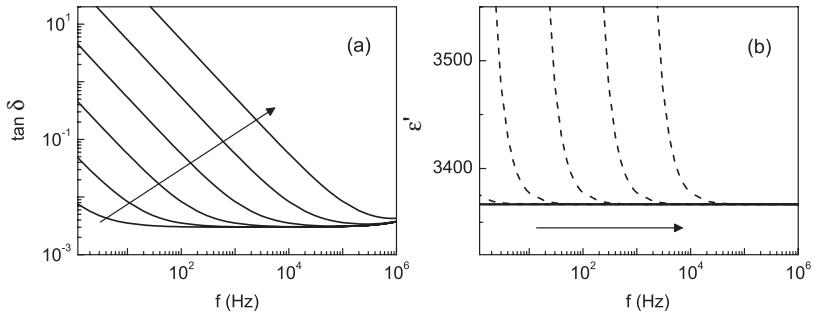

Figure 4. Effect of resistivity of FE film. The loss factor tan δ (a) and the permittivity ε' (b) as a function of frequency f estimated in FE thin-film heterostructure with FE thickness $d_F = 500$ nm, Pt electrode thickness $d_E = 100$ nm, and different FE resistivity $\rho_F = 10^4$–10^9 Ω m. The direction of decrease of ρ_F is shown by arrows. The dashed lines in (b) correspond to the assumption of the ideal capacitor.

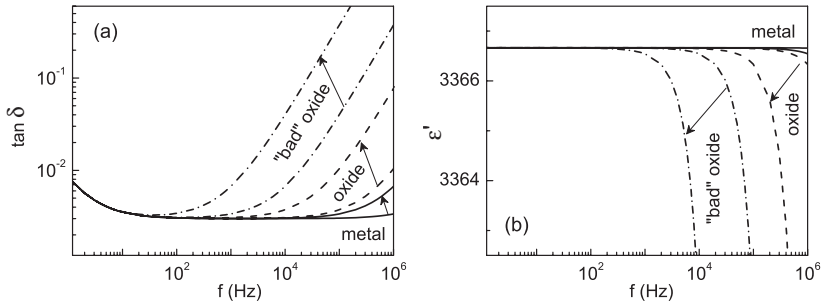

Figure 5. Effect of resistivity and thickness of the electrode layers. The loss factor tan δ (a) and the permittivity ε' (b) as a function of frequency f estimated in FE thin-film heterostructure with FE thickness $d_F = 500$ nm, electrode thickness $d_E = 100$ nm–1 μm, and different electrode resistivity $\rho_E = 10^{-7}$ (metal); 2×10^6 (oxide) and 10^{-4} Ω m ('bad' oxide). The direction of decrease of d_E is shown by arrows.

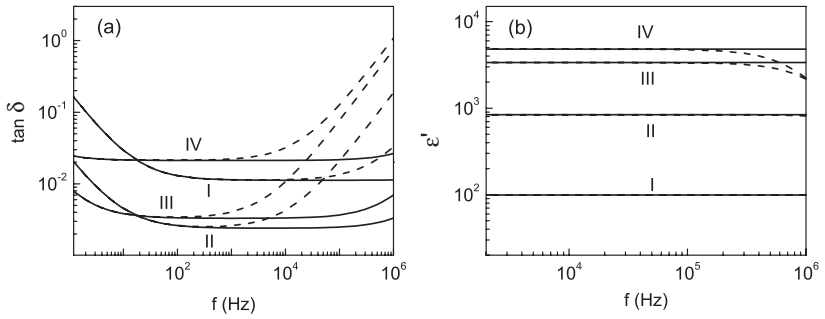

Figure 6. Effect of permittivity of FE film. The loss factor tan δ (a) and the permittivity ε' (b) as a function of frequency f estimated in FE thin-film heterostructure with FE thickness $d_F = 500$ nm, with Pt (solid lines) or oxide (dashed lines) electrodes of thickness $d_E = 100$ nm, and different FE permittivities $\varepsilon'_F = 100$ (curves I); 10^3 (curves II); 10^4 (curves III); and 10^5 (curves IV).

is clearly seen moves to lower frequencies (figure 6(a)). In a broad range of frequencies, the dependence of tan δ on ε'_F is nonmonotonic. With increasing permittivity ε'_F, the drop in the measured ε' becomes better expressed (figure 6(b)).

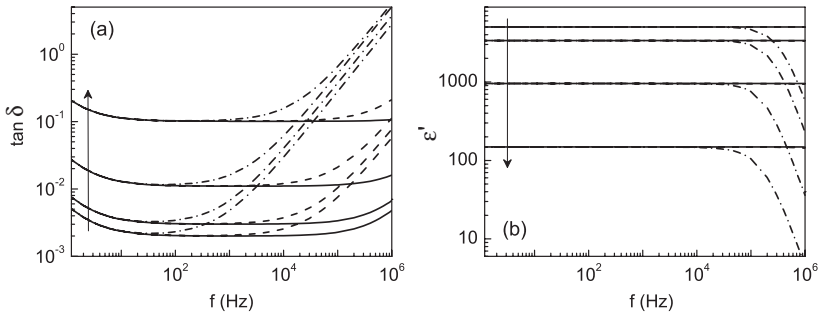

Figure 7. Effect of thickness of FE film. The loss factor tan δ (a) and the permittivity ε' (b) as a function of frequency f estimated in FE thin-film heterostructure with FE permittivity $\varepsilon'_{\mathrm{F}} = 10^4$, with Pt (solid curves) or oxide (dashed curves), or 'bad' oxide (dot–dash curves) electrodes of thickness $d_{\mathrm{E}} = 100$ nm, and different FE thickness $d_{\mathrm{F}} = 1000$; 500; 100; and 10 nm. The direction of decrease of d_{F} is shown by arrows.

With decreasing thickness d_{F} of FE film, the loss factor tan δ increases (figure 7(a)). The lowest frequency at which the corresponding decrease of the measured permittivity ε' becomes noticeable moves to lower frequencies (figure 7(b)).

The obtained frequency dispersion of the 'measured' dielectric properties of FE thin-film heterostructure (figures 4–7) can be modified by the frequency dependence of the dielectric permittivity of FE itself. The main tendencies, however, remain unchanged.

In thin-film FE even at low frequencies the loss factor is not directly related to the dielectric loss of FE. This makes the analysis of the imaginary part of the permittivity difficult, if not impossible. Also in the analysis of the real part ε' of the permittivity, the illustrated effects of size and properties should be taken into account. As an example, the dependence of the measured permittivity ε' on thickness d_{F} of FE film was considered in more detail.

In a heterostructure with high-resistivity electrodes, with decreasing thickness d_{F} of FE film, the measured loss factor tan δ increases (figure 8(a)) and the measured permittivity ε' decreases (figure 8(b)). Also with increasing frequency, tan δ increases (figure 8(a)), and ε' decreases (figure 8(b)). For FE thickness $d_{\mathrm{F}} = 200$ nm, such an electrode related frequency dependence of permittivity ε' is shown for the range of $f = 1$–100 kHz (figure 8(c)).

The frequency dispersion of ε' experimentally observed in both FE thin-film BST (figure 1(a)) and RFE thin-film PMN above T_{m} (figures 2(a) and (c)) was in good agreement with the estimated behaviour of $\varepsilon'(f)$ (figure 8(c)).

Thus, the initially assumed frequency dependence of permittivity $\varepsilon'_{\mathrm{i}}$ of the interface layer can be explained by the influence of the high-resistivity electrodes. However, similar frequency dispersion of ε' has been observed in thin-film heterostructures with low-resistivity (Pt) electrode layers [12]. This indicates an additional contribution to the resistance R_{E} from a source other than the electrode. One of the sources might be presented as a near-electrode layer of the FE possessing lower resistivity compared to that of FE film. Such a lower-resistivity layer can principally exist due to structural defects and stoichiometry deviations on the surface of perovskite FE. To separate different contributions—from the electrode or from such a layer—the frequency dependence of permittivity can be studied as a function of electrode thickness d_{E}.

The electrode related frequency dispersion of permittivity ε', which was revealed experimentally (figures 2(a) and (c)) and by estimations (figures 8(b) and (c)), can affect the character of the thickness dependence of permittivity $\varepsilon'(d_{\mathrm{F}})$ (figure 9(a)). Respectively, the slopes of the curves $1/\varepsilon' \propto 1/d_{\mathrm{F}}$, which are often used for determining the interface parameters

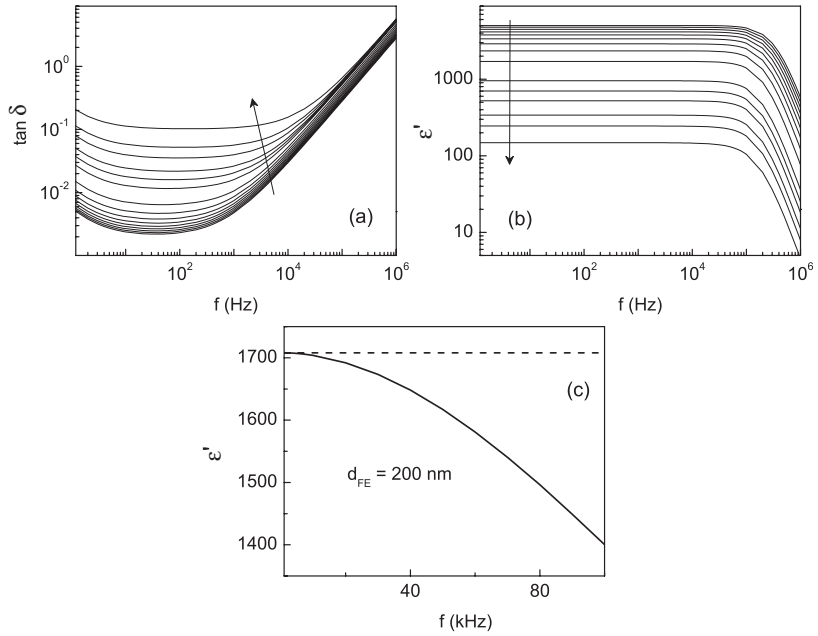

Figure 8. Effect of thickness of FE film with high-resistivity electrodes. The loss factor tan δ (a) and the permittivity ε' (b), (c) as a function of frequency f estimated in an FE thin-film heterostructure with FE permittivity $\varepsilon'_{\mathrm{F}} = 10^4$, with 'bad' oxide electrodes of thickness $d_{\mathrm{E}} = 100$ nm, and different FE thickness (b) $d_{\mathrm{F}} = 1000$–10 nm and (c) $d_{\mathrm{F}} = 200$ nm. The direction of decrease of d_{F} is shown by arrows. The dashed line in (c) shows the permittivity in the case of the low-resistivity electrodes.

$\varepsilon'_{\mathrm{i}}/d_{\mathrm{i}}$ (expressions (1) and (2)), vary with the measurement frequency (figure 9(b)). As seen (figure 9(c)), the effect of frequency on the behaviour of $1/\varepsilon'$ as a function of $1/d_{\mathrm{F}}$ is quite noticeable for typical experimental conditions: $d_{\mathrm{F}} = 100$–500 nm and $f = 0.1$–100 kHz.

Thus the results of estimations (figures 4–9) showed that in thin-film heterostructures of FE with the assumed frequency independent dielectric permittivity ($\varepsilon'_{\mathrm{F}}$, $\varepsilon''_{\mathrm{F}}$), the measured dielectric properties (ε', tan δ) can exhibit strong frequency dispersion depending on resistivity (ρ_{F} and ρ_{E}) and thicknesses (d_{F} and d_{E}) of both FE film and electrode layers, and on the permittivity $\varepsilon'_{\mathrm{F}}$ of FE film. Such a behaviour can be observed at frequencies as low as 100 Hz. Also this can explain the frequency dispersion of the permittivity $\varepsilon'_{\mathrm{i}}$ of the interface layer, suggested in the previous studies [5].

4. Frequency dependence of the dielectric permittivity in bulk relaxors

Since the discovery of RFEs, the nature of the dielectric relaxation in RFEs has been a subject of continuous research and discussion. Recently, experimental studies of the dielectric properties at frequencies from the millihertz range to the terahertz and infra-red range have been performed [13, 14]. In the low-frequency range, controversial results [13] have been obtained. Since the real part of the dielectric permittivity $\varepsilon'_{\mathrm{F}}$ of RFEs is very large, approaching 10^5 around T_{m}, the analysis of the measured dielectric response of RFE samples must include the above-described factors (see expression (10)).

To illustrate this, the low-frequency behaviour of the imaginary part ε'' of the permittivity was estimated using (10) and expressions (8) and (9), normally applied in the measurements of

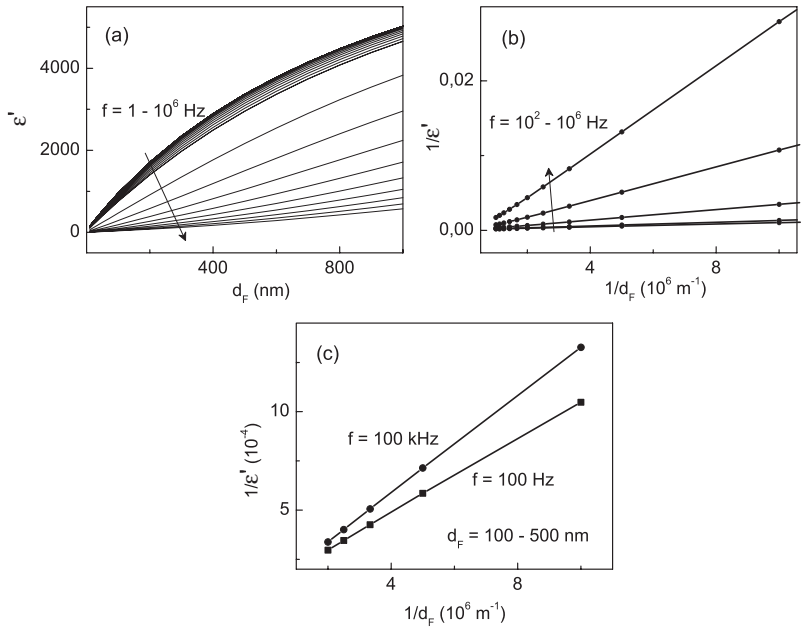

Figure 9. Effect of frequency on the measured thickness dependence of permittivity of FE film with high-resistivity electrodes. (a) The permittivity ε' as a function of FE thickness d_F at frequency $f = 1$–10^6 Hz. (b), (c) The inverse permittivity $1/\varepsilon'$ as a function of the inverse thickness $1/d_F$ at frequency $f = 1$–10^6 Hz. The direction of increase of f is shown by arrows. The estimations were performed for FE permittivity $\varepsilon'_F = 10^4$ and 'bad' oxide electrodes of thickness $d_E = 100$ nm.

bulk samples. The following parameters were taken into account:

$\varepsilon'_F = 500$; 1000; 10 000; 25 000; and 40 000 (depending, for example, on temperature);

$\varepsilon''_F = 1$; 10, 100, 500; and 1000; (corresponding to the above listed ε'_F);

$\rho_F = 10^{10}$ Ω m and 4–5 $\times$ 10^8 Ω m;

$d_F = 2 \times 10^{-4}$ m (0.2 mm);

$S = 10^{-6}$ m^2 (1 mm $\times$ 1 mm);

$f = 1$–10^6 Hz.

The contact resistance was assumed to be in the range $R_E = 1$–15 Ω. This could correspond to the presence of a lower-resistivity surface layer of a few nanometres in thickness.

The imaginary part (figure 10(a)) and the real part (figure 10(b)) of the estimated 'measured' permittivity of thick RFEs were in a good qualitative agreement with the reported experimental results [13]. At high temperatures, an increase of conductivity of RFEs could result in an apparent large ε'' below $f = 100$ Hz, and even an increase of ε', although the true ε'_F and ε''_F were assumed to be frequency independent parameters.

It should be noted that even in a 'good' RFE with large resistivity $\rho_F = 10^{10}$ Ω m the permittivity–resistivity pair could lead to an increase of ε'' with decreasing f below 1 Hz (curve 3 in figure 10(a)). Moreover, for the resistivity of RFE about 10^9 Ω m, such a permittivity–resistivity pair was found to result in a linear shape of the Cole–Cole plots for the permittivity (figure 11(a)). The obtained linear relation between ε' and ε'' might imitate a universal relaxation law.

For large $\varepsilon'_F = 25\,000$–$40\,000$ (often observed in RFE in the vicinity of T_m), with increasing frequency, a considerable increase of the measured ε'' (figures 10(a) and 11(b))

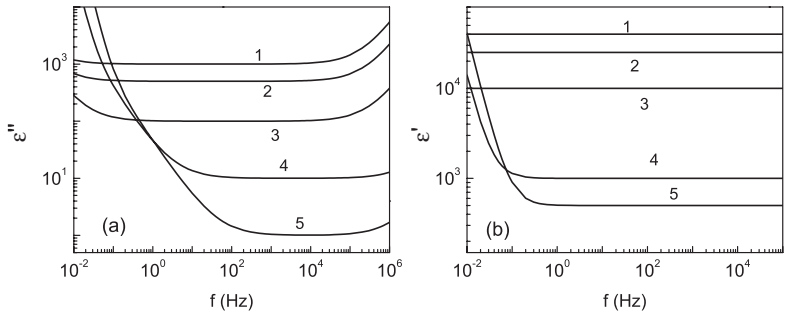

Figure 10. The imaginary part ε'' (a) and the real part ε' (b) of the dielectric permittivity as a function of frequency in bulk RFE heterostructure. The RFE resistivity is ρ_F is 10^{10} Ω m (curves 1, 2, and 3), 5×10^8 W m (curve 4), and 4×10^8 Ω m (curve 5).

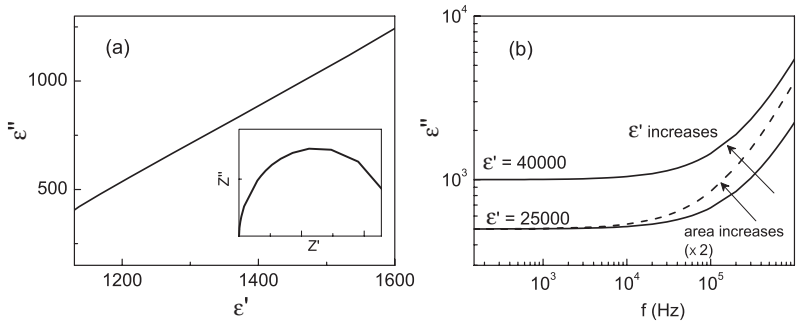

Figure 11. Effect of low resistivity of RFE and effect of capacitance in bulk RFE heterostructure. (a) The estimated Cole–Cole plot for the permittivity assuming $\rho_F = 10^9$ Ω m. The corresponding impedance is shown in the inset. (b) The imaginary part ε'' of the dielectric permittivity as a function of frequency. The direction of increase of capacitance is shown by arrows (b).

was obtained, while the measured ε' remained unchanged (figure 10(b)). The character of the dependence $\varepsilon''(f)$ above 10 kHz was not much affected by size variations (figure 11(b)). In a PMN single crystal around the dielectric maximum, such an increase of ε'' in the frequency range of 10–100 kHz has been observed experimentally [14]. Fortunately, the measurements have been performed in a very broad frequency range and using different techniques that allowed the authors to ignore the uprising tails of ε''.

A closer inspection of the dependence $\varepsilon''(f)$ determined by the contact resistance R_E (figure 12(a)) revealed a good fit to the power law $\varepsilon'' \propto f^m$. The exponent m was found to increase with increasing R_E. For fixed R_E, the exponent m was a function of the real part of permittivity $\varepsilon' = \varepsilon'_F$ (figure 12(b)): with increasing ε', the exponent m considerably increased. Also with increasing ε', the lowest frequency at which the behaviour $\varepsilon'' \propto f^m$ became dominating was moving to lower frequencies. The frequency normalization $f_n = n \cdot f$ was performed with the normalization parameter $n = 1$ for $\varepsilon' = 500$. After applying the frequency normalization for all dependences $\varepsilon''(f)$ (from figure 12(b)), a single 'master' curve $\varepsilon''/\varepsilon''_F \propto (f_n)^m$ was obtained (figure 13(a)). The normalization parameter n increased with increasing permittivity ε' (figure 13(b)). Assuming the temperature dependence of the permittivity $\varepsilon'(T)$, the temperature dependence of both the exponent m (figure 12(b)) and the normalization parameter n (figure 13(b)) can be shown.

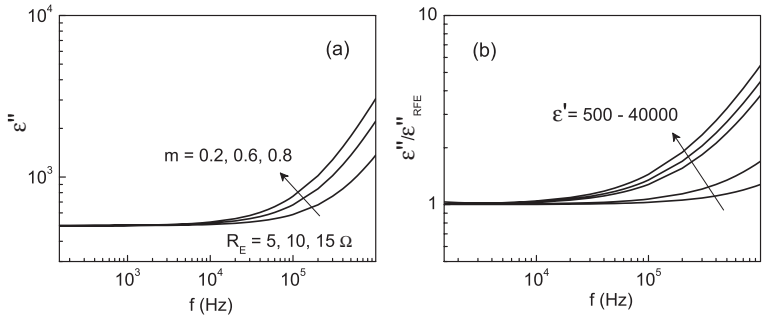

Figure 12. The imaginary part ε'' of the dielectric permittivity as a function of frequency in bulk RFE heterostructure. The effect of the contact resistance R_E (a) and the effect of the real part ε' of permittivity (b). The direction of increase of parameters is shown by arrows.

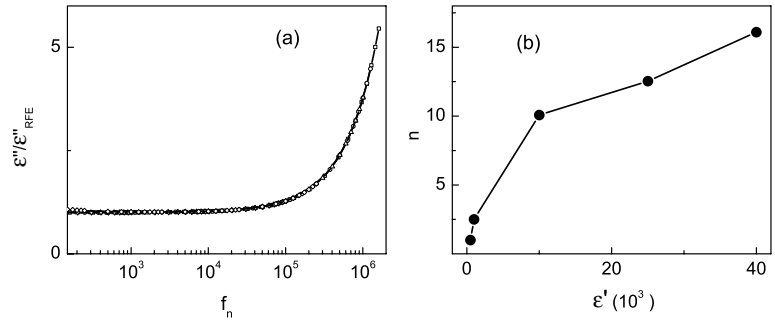

Figure 13. 'Dispersion law' in bulk RFE heterostructure. (a) The ratio of the normalized imaginary part ε'' of the permittivity in the heterostructure to that ε''_{RFE} in RFE as a function of the normalized frequency f_n. All curves obtained for different permittivities of RFE merge into one 'master curve'. (b) The normalization parameter n as a function of the real part ε' of the permittivity of RFE.

Thus the presence of the contact resistance R_E can dramatically affect the measured low-frequency dielectric response of the bulk RFE. According to the experimental results obtained for a PMN crystal [14], the magnitude of R_E can be a few ohms. Such a value could easily lead to the additional relaxation law $\varepsilon'' \propto (nf)^m$ and its temperature evolution, with the temperature dependent parameters m and n.

Good agreement between the estimated and experimentally observed dielectric properties was found for the resistance R_E being hundreds of ohms in FE thin-film heterostructures, and a few ohms in bulk RFE samples. For both the thin-film and bulk capacitors the corresponding (resistance $\times$ area) factor was in the range of $(R_E \times S) = 10^{-6}$–10^{-5} Ω m^2. This similarity could indicate a common source of R_E, such as, for example, the above-suggested lower-resistivity layer near the electrode. The resistivity of the 1–10 nm thick near-electrode layer might be in the range of 10^2–10^3 Ω m, respectively. More studies would be desirable to clarify the origin of the large R_E in thin-film and bulk RFE/FE.

In conclusion, the low-frequency dielectric response of thin-film and bulk perovskite FE/RFE was analysed using the comparison of the experimental results with the results of estimations. The combined effects of properties and thicknesses of both FE/RFE and electrode layers on the dielectric response was demonstrated. In thin-film FE/RFE, more data in support of the interface model were obtained. The dielectric dispersion and large losses were explained as originating from the joint film–electrode scaling. An experimental study of the interface

parameters using the thickness dependence of the permittivity was shown to be incorrect. In bulk RFE, the RFE–electrode pair was found to give additional relaxation laws, which are not related to the true dielectric relaxation in RFE. Both in thin-film FE/RFE and bulk RFE, a lower-resistivity layer was suggested to exist at the surface of perovskite FE/RFE.

Acknowledgments

The author expresses her gratitude to J Levoska and I Jaakola for discussions and assistance in the manuscript preparation. The author wishes to thank the organizers and participants of the COST 528 Workshop, November 2005, Prague, for their encouragement of the work.

References

[1] Dawber M, Rabe K M and Scott J F 2005 *Rev. Mod. Phys.* **77** 1083
[2] Miller S L, Nasby R D, Schwank J R, Rodgers M S and Dressendorfer P V 1990 *J. Appl. Phys.* **68** 6463
[3] Vendik O G and Zubko S P 2000 *J. Appl. Phys.* **88** 5343
[4] Pertsev N A, Artl G and Zembilgotov A G 1996 *Phys. Rev. Lett.* **76** 1364
[5] Tyunina M and Levoska J 2001 *Phys. Rev.* B **63** 224102
[6] Tyunina M and Levoska J 2004 *Phys. Rev.* B **70** 132105
[7] Tyunina M and Levoska J 2005 *J. Appl. Phys.* **97** 114107
[8] Sinnamon L J, Bowman R M and Gregg J M 2001 *Appl. Phys. Lett.* **78** 1724 and references therein
[9] Bokov A A, Bing Y H, Chen W, Ye Z G, Bogatina S A, Raevski I P, Raevskaya S I and Sahkar E V 2003 *Phys. Rev.* B **68** 052102
[10] Moriya Y, Kawaji H, Tojo T and Atake T 2003 *Phys. Rev. Lett.* **90** 205901
[11] Lu T and Cao W 2002 *Phys. Rev.* B **66** 024102
[12] Kighelman Z, Damjanovic D and Setter N 2001 *J. Appl. Phys.* **89** 1393
[13] Bokov A A and Ye Z G 2002 *Phys. Rev.* B **65** 144112
[14] Bovtun V, Kamba S, Pashkin A, Savinov M, Samoukhina P, Petzelt J, Bykov I P and Glinchuk M D 2004 *Ferroelectrics* **298** 23